

Surface wave dynamics off Mumbai coast, north-eastern Arabian Sea

V. Sanil Kumar^{1*}, Jesbin Geroge¹, Udhaba Dora², Naseef Muhamed¹

¹Ocean Engineering, CSIR-National Institute of Oceanography
(Council of Scientific & Industrial Research), Dona Paula, Goa 403 004 India

² CSIR-National Institute of Oceanography Regional Centre Mumbai, Lokhandwala Road, Four Bungalows, Andheri (W), Mumbai - 400 053, India

*corresponding author Tel: 0091 832 2450 327 email:sanil@nio.org

Abstract

Directional wave data collected in the coastal area at 10-m water depth for a period of one year is used to describe the surface wave dynamics off Mumbai coast. Partitioning of the wave spectrum into locally generated waves and remotely generated swells indicate that annually 57% of the surface height variance in the study area is a result of wind-seas and the remainder are swells from the southwest. More energetic waves are dominantly young swells and are observed during Indian summer monsoon (June-September), often generated by Somali jet. The waves are also occasionally influenced by the stronger winds over the south Indian Ocean and the Southern Ocean. The wave data indicate that the north-eastern Arabian Sea has two predominant wave regimes; i) swells with peak wave period > 10 s from the southwest and ii) wind-seas with peak wave period < 8 s from the northwest. In the pre-monsoon (February-May) the spectral density of the sea surface height variance of the wind-seas are higher than that of the swells. The direction of wind-seas and swells differ by 37 to 79° during the non-monsoon period, whereas it is less than 23° during the summer monsoon.

Key Words: Multi-peaked spectra, wind-seas, swells, wind waves, Indian Summer monsoon, ocean sciences

1. Introduction

The surface waves generated by winds with periods ranging from 2 to 25 s are of importance to scientific and practical aspects (Chakrabarti 2005). Waves play an important role in the coastal erosion and accretion (Dean and Dalrymple 2002). The waves propagate out of the generation areas travel over a great distance across the ocean and enter the coastal regions (Munk et al. 1963). Hence, the wave characteristics at a location are composed of a number of wave types, originating from a range of synoptic weather systems that produce distinct surface wind-wave signatures (Holthuijsen 2007). The surface wave field of a region is a result of the combination of local and remote forcing. One of the largest challenges at most locations is the lack of observations, which hampers wave dynamics studies and wave model development.

The Arabian Sea is a semi-enclosed basin in the northern hemisphere and is part of the North Indian Ocean (Fig. 1). There are few observational and modelling studies that have been performed to describe wave characteristics in the eastern Arabian Sea (see Amrutha and Kumar 2017 for review). Most of these studies examined the wave characteristics in the central west coast of India. The earlier studies along the eastern Arabian Sea reported that the seasonal average wave height and period did not vary significantly between the stations spaced at 350 km (Kumar et al. 2012; Kumar et al. 2014; Anoop et al. 2014). Multi-modal spectra is another common feature in the eastern Arabian Sea due to the co-existence of wind-sea (waves forced by local wind) and swells (waves forced remotely). The earlier studies indicate that the waves in the Arabian Sea are predominantly swells (Kumar and Anand 2004; Glejin et al. 2013), but the contribution of wind-seas and swells to the waves in the eastern Arabian Sea vary during different periods of the year (Anjali and Kumar 2016). The separate analysis of wind-sea and swell contributions to significant wave height (H_s) provides a better understanding of the factors that determine the variability of the wave field. The summer monsoon (June-September) onset is characterized by rapid changes in the prevailing rainfall intensity and wind direction and generally arrive in the Arabian Sea by the first week of June (Joseph et al. 2006). Advancing through the Arabian Sea, by 10 June it touches the Mumbai coast. During the summer monsoon, due to the strong cross-equatorial monsoon low-level jets also known as Somali (Findlater) Jet (Findlater 1969), wave heights are high in the Arabian Sea (Anoop et al. 2015).

Mumbai with a population of 112 million in an area of 307713 km² is the financial capital of India (Census 2011). To provide better connectivity, sea links and coastal roads on a reclaimed area is planned and the wave characteristics form the basic input for designing these structures. No studies reported on the characteristics of the waves in the northeastern Arabian Sea. In this article, we studied the influence of local wind on the wave characteristics at a location in 10 m water depth in

the northeastern Arabian Sea (Fig. 1). Our study is based on year-long measurements (January-December 2017) carried out using moored directional waverider buoy.

2. Materials and methods

Wave data measured using the Datawell directional waverider buoy (Datawell, 2009) is used in the study. The raw wave data are stored in the internal memory of buoy and retrieved during annual maintenance. The displacement of the buoy is sampled continuously at a rate of 3.84 Hz and are transmitted and recorded on-board with a sampling frequency of 1.28 Hz and the data for every 30 minutes are processed as one record. There are no data gaps and a total of 17,520 data records covering one-year period are analysed. A pronounced peak of the spectral density at the low-frequency side of the spectrum raises the suspicion that the stabilized platform suspension is out of order and can be a spurious data (Datawell, 2009). Checked for spectral peaks that are orders of magnitude higher than $10^{-2} \text{ m}^2 \text{ Hz}$ in the frequency range (0.025-0.035 Hz) and found that such peaks are present in 2 records and these data are not used in further analysis. Wave data analysis is performed both in the time and frequency domain. In the time domain, each individual wave is selected based on the zero-crossing method and the maximum wave height (H_{\max}) is computed. The details of the data collection and analysis are presented in Kumar et al. (2014). Significant wave height (H_s) and the mean wave period (T_{m02}), are obtained from the spectral moment. The high-frequency response of the wave buoy is limited by the dimensions of the buoy. For wavelengths smaller than the buoy's circumference, the wave motion is not followed anymore by the buoy and can introduce noise. Hence, all outputs of the buoy sensors are filtered by applying a low-pass filter with 0.58 Hz cut-off frequency. Hence, data with frequency ranging from 0.025 to 0.58 Hz is only used in the analysis. The frequency resolution is 0.005 Hz for frequencies less than 0.1 Hz and it is 0.01 Hz from 0.1 to 0.58 Hz. Since the wave spectrum referred in this article is the distribution of wave energy (or variance of the sea surface height) over frequency, the terminology spectral density of the sea surface height variance is used. Spectral peak period (T_p) is the inverse of the frequency at which the wave spectral density of the sea surface height reaches its maximum. Mean wave direction (θ_m) corresponding to the spectral peak and the directional spread are estimated based on circular moments (Kuik et al. 1988). The direction represents where the waves come from; 0° means waves are coming from the north, 90° waves from the east, and so on. Time referred in the paper is Coordinated Universal Time (UTC). The 1-D separation algorithm (Portilla et al. 2009) is used to separate the wind-seas and swells and is on the hypothesis that, the spectral density of the sea surface height variance at the peak frequency of a swell cannot be higher than the value of a Pierson-Moskowitz (PM) spectrum (Pierson and Moskowitz 1964) with the same frequency. If the ratio

between the peak spectral density of the sea surface height variance of a wave system and that of a PM spectrum at the same frequency is above a threshold value of 1, the system is considered to represent wind-sea, else it is taken to be swell. A separation frequency f_c is estimated following Portilla et al. (2009) and the swell and wind-sea parameters are obtained for frequencies ranging from 0.025 Hz to f_c and from f_c to 0.58 Hz, respectively. It is noted that the shoreline orientation of the region is nominally 8° counter-clockwise from N-S. Directional spectrum of surface wave field $E(f, \theta)$ represents the spectral density of the sea surface height variance at each frequency (f) and direction (θ). H_s associated with particular frequency band (f_1 to f_2) and direction band (θ_1 to θ_2) is

estimated as $H_{s_1} = 4 \sqrt{\int_{f_1}^{f_2} \int_{\theta_1}^{\theta_2} E(f, \theta) df d\theta}$. H_s associated with swells ($f_1=0.025$, $f_2=f_c$) and wind-seas

($f_1=f_c$, $f_2=0.58\text{Hz}$) are separated and the waves from direction bands $0-168^\circ$ (representing waves from the land direction i.e. the reflected waves and the waves generated due to land breeze), $168-248^\circ$ (representing waves from south Indian Ocean and Southern Ocean which cause northerly littoral drift), $248-280^\circ$ (waves from west) and $280-360^\circ$ (representing waves from northwest which cause southerly littoral drift) are presented. From the wave spectrum measured at half-hourly interval, the monthly averaged wave spectrum is computed by averaging the spectral density of the sea surface height variance at the respective frequencies over the specified time.

The new ECMWF (European Centre for Medium-Range Weather Forecasts) climate reanalysis data (ERA-5) is used to examine the latitudinal distribution of the significant wave height and the peak wave period and the wind roses at different locations in the Arabian Sea. ERA-5 is the fifth generation of ECMWF atmospheric reanalyses of the global climate and it provides hourly estimates of the variables on a 30 km grid.

3. Results and discussions

3.1 Bulk wave parameters

Half-hourly time series data of the H_s is presented in Fig. 2a. The wind-sea dominated or swell dominated sea states are presented separately based on the peak wave period (T_p). Wave field with $T_p < 8$ s is likely wind-driven, whereas $T_p > 8$ s likely indicates the dominant presence of swell waves. Mostly wind-sea predominance is observed during January to May and from September to December except during the high-wave events. During June and July, only swell predominance is observed. Over the one-year period, 69% of the time, swell dominance is found. Monthly averages of the H_s are presented in Fig. 2a. The lowest waves are found in January with monthly mean H_s values of ~ 0.5 m. The waves progressively increase in height from January and reach the highest value

(~3.6 m) in June with a monthly average H_s of 1.9 m and then decrease in height and reach the lowest monthly average (~0.4 m) in November (Fig. 2a). High waves ($H_s \sim 1.5$ to 2.5 m) observed during 4-5 December 2017 is due to the tropical cyclone Ockhi which originated in the eastern Andaman Sea on 21 November 2017 and dissipated near the south coast of Gujarat on 6 December 2017. The wave height exhibited greater values than the annual mean (~0.91 m) during the monsoon months (June-September) and smaller values than the annual mean during the rest of the year. During June and July, the H_s is always greater than 1 m. Partitioning of the wave spectrum into locally generated waves and remotely generated swells based on partition algorithm indicate that the swell H_s varies from 0.2 to 3.2 m with a mean of 1.2 m during the monsoon and that due to wind-sea are from 0.1 to 2.5 m with mean of 0.8 m. During the non-monsoon, swell H_s varied from 0.1 to 2.4 m with a mean of 0.3 m and the wind-sea H_s varied from 0.1 to 1.4 m with a mean value of 0.5 m. In general, the amplitude of the annual mean (0.61 m) wind-sea H_s is comparable to that (0.62 m) of the swell H_s . The annual mean H_s for the study area is slightly less than that (~ 1-1.1 m) reported for other locations in the eastern Arabian Sea (Sajiv et al. 2013; Kumar et al. 2014) due to the decrease in the swell H_s .

The H_{max} varied from 0.3 to 5.7 m with an average value of 1.4 m. Since the waves are measured in the nearshore waters, the crest height is more than the trough height. The crest heights of the individual wave in a 30-minute record vary from 0.56 to 0.86 times the wave height with an average value of 0.6. In the same 30-minutes record, the crest heights more than 3 m is 1.0 to 1.6 times the H_s of the same 30-minutes data.

The variation of mean wave period over an annual cycle is 2.4 to 8.9 s with the mean value of 4.6 s. Waves are with low mean wave period during January to March with average values of 3.8 s and the wave period is relatively high during June (Fig. 2b). Largest mean wave period (~8.9 s) is during the tropical cyclone Ockhi, whereas the highest value during the monsoon is 8.6 s. Wide range (2 to 22 s) is observed in the peak (most energetic) wave period with a mean value of 10 s indicating that the wave regime of the study area consists of short to long-period waves. Compared to H_s , the T_p displays a large temporal variability within one month period (Fig. 2c). The occurrence of these short-term shifts in T_p with negligible variation in H_s is due to the presence of two wave regimes (swells and the wind-sea) and the predominance of one over the other. Lowest T_p occurs during April with a monthly average value of 7.8 s due to the larger presence of wind-seas compared to other seasons (Fig. 2c). Highest T_p (monthly average value of 12.1 s) is during October when long-period swells with relatively small wave heights ($H_s < 1$ m) are predominant (Fig. 2c). During the monsoon months, even though strong wind forcing is present, the smaller T_p values do not occur

in because of the larger presence of young swells. Long-period waves with T_p more than 15 s are observed during 21, 16, 15, 15% of the time in March, October, May and December and these waves are with H_s less than 1 m except during 1% of the time in May.

Long-period waves ($T_p > 18$ s) with significant energy arrive at the study area with a gap of 6 to 8 days. 1.8% of the time in 2017, waves with $T_p > 18$ s and 8.4% of the time, $T_p > 15$ s are observed. Long-period waves with H_s varying from 0.8 to 1.1 m are recorded in May. Long-period waves are from 210 to 260°. During the monsoon, even though long-period waves are present, they are not predominant and only two records with $T_p > 18$ s are observed in this season and these waves are with relatively higher heights ($H_s \sim 1.6$ m) compared to the long-period waves in the non-monsoon period. In the eastern Arabian Sea, Glejin et al. (2016) observed low-amplitude long-period swells ($T_p > 18$ s) during 1.4 to 3.6% of the time in a year, and these waves were mainly during the non-monsoon period.

In order to examine the source of the long-period waves, the latitudinal distribution of the H_s and T_p along 70.2° E longitude is presented (Fig. 3). The wind speed in the Southern Ocean frequently goes beyond 14 m/s (Fig. 3a) and generates high waves ($H_s > 5$ m). These high waves travel and reach the north Indian Ocean in 5 to 6 days and result in long-period waves (Fig. 3c). While propagating through the Indian Ocean, these long-period waves lose most of its energy and result in waves with $H_s < 1$ m (Fig. 3b). Earlier Amrutha et al. (2017) reported that the high waves ($H_s > 4$ m) generated in an area bounded by 40-60° S and 20-40° E in the south Indian Ocean reached the eastern Arabian Sea in 5-6 days and resulted in the long-period swells.

The mean peak direction (D_p) values are mainly from SW-W, but due to the bimodal characteristics of waves in this region, the high-frequency waves are from NW when the wind-sea is predominant (Fig. 2d). In the study area, the swell generally comes from the SW and wind-sea varies from NW under the influence of the Shamal wind and from SW-W in the active monsoon period. Waves from S to W (180-270°) are predominantly swell waves. Waves with H_s more than 1 m during January to April are from N-NW (290-340°).

To provide an overview of wave statistics, we group our results in pre-monsoon (February-May), monsoon, post-monsoon (October-January) seasons and presented the wave rose diagrams (Fig. 4). Swell waves have larger amplitudes during monsoon and smaller amplitude during the non-monsoon period. The seasonal mean H_s indicate large seasonal variations in wave height. Smallest H_s values occur in post-monsoon with seasonal average value of 0.5 m, whereas during the pre-monsoon the waves are slightly higher in magnitude with seasonal average value of 0.7 m and that

during the monsoon is 1.5 m. For waves with $H_s > 0.5$ m, swell waves contribute substantially to overall wave energy. More energetic waves ($H_s > 2.5$ m) are dominantly young swells ($T_p \sim 10$ to 13.3 s) from 233-255° and are observed during monsoon. 10 to 14 s waves are resulting from wind speed of 15 to 18 m/s (Pierson and Moskowitz 1964 Wind rose at 12.9° N; 59.1° E, Somalia offshore shows strong wind (12 to 16 m/s) from 210-240° during June-September, which generates 10 to 14 s waves and these waves propagate and reach the eastern Arabian Sea (Fig. 5). Even in the study area and in the central Arabian Sea during June-September, the wind is from south-west during 70% of the time, but the wind speed is 4 to 12 m/s (Fig. 5). Hence, the wind-seas and the young swells are also from south-west during the monsoon period. In the post-monsoon and the pre-monsoon period, the winds offshore of Somalia is not contributing to the waves in the study area.

Seasonal changes in the mean wave period are associated with the presence of wind-sea conditions, which are characterized by shorter periods. The wind rose near the buoy location in the pre-monsoon period indicate that the during 70% of the time, wind is from 270 to 360° with speed up to 8 m/s. The seasonal average of the T_p is highest (10.5 s) during the post-monsoon due to the presence of long-period swells and is lowest (~8.9 s) during the pre-monsoon due to the larger presence of wind-seas. During the monsoon, the waves are from a narrow band (225-247.5°) resulting in uni-modal distribution, whereas during pre-monsoon, waves are from a wider range, 180 to 337.5° (Fig. 4). During the post-monsoon, most of the time, in the study area winds are from 330 to 30° with speeds up to 8 m/s and hence, when the wind-sea contribution to the wave spectral density of the sea surface height variance is more, the waves are from 315 to 337.5° (Fig. 4). In the pre-monsoon, 74% of the surface height variance is a result of wind-seas (Fig. 2e). During pre-monsoon, the sea state off the Mumbai coast is dominated by short-period, locally generated waves up to 55% of the time. Whereas during the post-monsoon, swells dominates up to 68% of the time and in the monsoon swell domination is up to 96%. In an annual cycle, 57% of the surface height variance in the study area is a result of wind-seas from the southwest (26.4%), west (18.9%) and north-west (11.7%) and the remainder are swells from the west (14.4%) and southwest (28.6%). The wave rose diagram indicates that the study area has 2 predominant wave regimes; i) swells ($T_p > 10$ s) from the southwest and ii) wind-seas ($H_s < 1.5$ m & $T_p < 8$ s) from the northwest.

The sea and land breeze combination is a feature observed in the coastal areas of the subtropics and tropics (Miller et al. 2003). Over the study area during most of the time, the wave climate is characterized by sea-land breeze structure and is feeble during the monsoon period (Fig. 6). The waves are under the control of wind-sea generated by sea-breeze in a diurnal pattern with the

maximum height during late evening (1730-2330 LT i.e. 1200-1800 GMT) and the minimum during the early morning (0200-0600 GMT) and is similar to that reported over the central west coast of India (Glejin et al. 2013). Figure 6 also shows an inverse relation between the wave periods (both the mean wave period and the peak wave period) and the wave height.

3.2 Wave spectral parameters

Over a period of one-year, the wave spectra have two, three or more peaks with the low-frequency band containing significant spectral density of the sea surface height variance. The spectral density of the sea surface height variance distribution of waves over a range of frequencies with time is studied by plotting the normalised wave spectral energy density in the time-frequency frame (Fig. 7a). Each wave spectrum is normalized by the maximum spectral density of the sea surface height variance of the respective spectrum. The maximum spectral density of the sea surface height variance used for normalisation is presented in Fig. 2f. The normalized spectral density of the sea surface height plots in the time-frequency field indicates the predominance of spectral energy in frequency bands 0.06-0.09 Hz (corresponding to swells) during the monsoon period. During the pre and post-monsoon, predominantly spectral energy is also in 0.18-0.24 Hz (corresponding to wind-seas) (Fig. 7a). During the monsoon, the direction of wind-sea and swell are similar with the difference up to 23°. Whereas, during the pre and post-monsoon, the average difference in wave direction of wind-sea and swell was large (37 to 79°) (Fig. 7b) and therefore it is important to consider the direction of wind-sea and swell while planning marine operations along the eastern Arabian Sea during the pre and post-monsoon. The directional spread (directional width) at spectral peak of waves with $H_s > 1$ m, which are predominantly swells is less with average value of 13° compared to the annual average of 21°. For long-crested waves (i.e. waves with long crest), the value of directional width is close to 0° and as the waves become short-crested, the directional spreading increases. In deep water, swell can be fairly regular and long-crested. The directional width is smallest for peak frequency and increases at frequencies lower and higher than the peak (Fig. 7c). Increase in directional width is higher for the lower frequencies compared to higher frequencies. During the monsoon, the directional spread is minimum and relatively large values are observed during the non-monsoon period due to the co-existence of swells and wind-seas. Occasionally significant spectral energy is observed from different directions (Fig. 7d). Directional bimodality is also observed with same frequency waves arriving from different directions.

Measured data consists of single-peaked swell, single-peaked wind-sea and swell or wind-sea dominated multi-peaked spectra (Table 1). A majority of the data recorded are multi-peaked spectra (69.5% of the time) and the multi-peaked spectra are swell dominated during 40.1% of time and

wind-sea dominated during 22.1% of the time. The single-peak spectra are mainly swell dominated (~29.5% time). More multi-peaked spectra are observed in the present study area compared to that (~37 to 54%) observed along the central west coast of India (Kumar et al. 2014).

Monthly averaged wave spectra were single-peaked during June to September with peaks around 0.09-0.1 Hz and they were double-peaked during remaining months (Fig. 8). For the double-peaked spectra, the primary peak during January to April is due to wind-sea and is at 0.16 to 0.22 Hz, whereas the primary peak during May, October to December is due to the long-period swells and is at 0.08 to 0.1 Hz (Fig. 8). The secondary peak of the double-peaked spectra is due to wind-seas during May, October to December and during other months it is due to wind-seas. The spectral density of the sea surface height variance at the primary spectral peak is least ($0.02 \text{ m}^2/\text{Hz}$) in January with monthly average value of $\sim 0.103 \text{ m}^2/\text{Hz}$ and it reaches the peak ($33.18 \text{ m}^2/\text{Hz}$) in June with monthly average value of $4.309 \text{ m}^2/\text{Hz}$. Almost equal spectral density ($\sim 0.1 \text{ m}^2/\text{Hz}$) is observed in February at the primary and secondary peak. The spectral density of the sea surface height variance at swell peak is almost double that of the wind-sea during October to December (Table 2). Narrow banded distinct swells of frequency in excess of 15 s are present along with one predominant swell peak and a wind-sea peak during March, May, October and December.

The seasonal variation in the wave spectrum (Fig 9) is seen as a broad region of higher wave spectral energy in the W–NW direction at frequencies between 0.16 and 0.2 Hz in the pre-monsoon compared to post-monsoon period, whereas no significant change in the swell spectral energy density is observed between these two seasons except in May. In the pre-monsoon compared to the post-monsoon, the spectral energy density is higher by $0.15 \text{ m}^2/\text{Hz}/\text{Rad}$ for frequencies 0.16 to 0.2 Hz and for directions between $270\text{-}330^\circ$, which indicates that north-west wind-seas are higher during the pre-monsoon. Another possible source of seasonal variability is the change in the direction of the 3 s wind-seas in March and April ($\sim 270\text{-}290^\circ$) compared to that ($\sim 300\text{-}320^\circ$) during November to February.

H_s associated with swells ($f_1 = 0.025$, $f_2 = f_c$ Hz) and wind-seas ($f_1 = f_c$, $f_2 = 0.58$ Hz) are separated in different direction bands and are presented in Fig. 10. 24% of the sea surface height variance in a year is a result of wind-seas from 280 to 360° and 24% are the swells from the southwest. In a year, 23% are wind-seas from 248 to 280° and 11% are the swells from the same directional sector. The waves from 0 to 168° are the waves approaching the buoy location from the coast and in a year these waves contribute $\sim 4\%$ of the sea surface height variance. The wave from the coast is partly due to the land breeze and partly are the reflected waves (Anoop et al. 2014).

4. Conclusions

This study analyzes a one-year record of surface wave data collected off Mumbai coast at 10 m depth in the Arabian Sea. A partitioning analysis of the wave height spectrum reveals swell and wind-driven waves. The most energetic waves occur during the monsoon period (June to September) as swell waves and these waves are driven by monsoon winds. During the non-monsoon period, both swells and wind-seas substantially contribute to the wave energy, but the area is relatively calm with significant wave height (H_s) less than 1 m. The waves are influenced by the winds from the northwest and the stronger winds over the south Indian Ocean and the Southern Ocean. During the pre-monsoon period, due to the strong local winds and the swells arriving from the south Indian Ocean and the Southern Ocean, more double-peaked spectra are observed. The double-peaked spectra are usually swell-dominated during the post-monsoon period, whereas it is wind-sea dominated during the pre-monsoon period. In the pre and post-monsoon seasons, significant difference of 37 to 79° is observed between the predominant directions of the wind-seas and swells.

Acknowledgments

The authors gratefully acknowledge the financial support given by the Council of Scientific & Industrial Research, New Delhi and Earth System Science Organization, Ministry of Earth Sciences, Government of India to conduct this research. We thank Dr. T. M. Balakrishnan Nair, Head of the Ocean Science & Information Services Group, INCOIS, Hyderabad. We thank Mr. Arun Nherakkol, a scientist with INCOIS and Mr. Jai Singh, technical assistant at CSIR-NIO, for the help during data collection. We thank the reviewer and the Editor for the suggestions which improved the scientific content of this paper. This is NIO contribution No. ----. The data used in this study is available at INCOIS (http://www.incois.gov.in/Incois/info_insitu.jsp).

References

- Amrutha MM, Sanil Kumar V (2017) Observation of dominance of swells over wind seas in the coastal waters of the Gulf of Mannar, India, *Ocean Science* 13: 703–717, doi: 10.5194/os-13-703-2017.
- Amrutha MM, Sanil Kumar V, Jesbin George (2017) Observations of long-period waves in the nearshore waters of central west coast of India during the fall inter-monsoon period, *Ocean Engineering* 131: 244-262, 10.1016/j.oceaneng.2017.01.014.
- Anjali Nair M, Sanil Kumar V (2016) Spectral wave climatology off Ratnagiri - northeast Arabian Sea, *Natural Hazards* 82: 1565-1588. doi:10.1007/s11069-016-2257-5.
- Anoop TR, Kumar VS, Shanas, PR, Johnson G (2015) Surface wave climatology and its variability in the North Indian Ocean based on ERA-Interim reanalysis. *Journal of Atmospheric and Oceanic Technology* 32: 1372-1385. doi: 10.1175/JTECH-D-14-00212.1, 2015.

Anoop TR, Sanil Kumar V, Shanas PR (2014) Spatial and temporal variation of surface waves in shallow waters along eastern Arabian Sea. *Ocean Engineering* 81: 150-157, doi: 10.1016/j.oceaneng.2014.02.010.

Census (2011) District Census Handbook Mumbai, Census of India 2011 Maharashtra Series 28, Part XII-B, Directorate of Census Operations, Maharashtra Ministry of Home Affairs, Maharashtra Exchange Building, 2nd Floor, Sir Shivasagar Ram Gulam Marg, Mumbai. (http://censusindia.gov.in/2011census/dchb/2723_PART_B_DCHB_%20MUMBAI.pdf) Accessed on 5 May 2018.

Chakrabarti SK (2005) Handbook of Offshore Engineering, Vol-1, Ocean Engineering Series, Elsevier, p 661

Datawell (2009) Datawell Waverider Reference Manual, Datawell BV oceanographic instruments, The Netherlands, pp 123.

Dean RG, Dalrymple RA (2002) Coastal Processes - With Engineering Applications, Cambridge Univ. Press, <https://doi.org/10.1017/CBO9780511754500>.

Findlater J (1969) A major low-level air current near the Indian Ocean during the northern summer. *Quart J Roy Meteor Soc* 95: 362-380.

Glejin J, Kumar VS, Nair TNB, Singh J (2013) Influence of winds on temporally varying short and long period gravity waves in the nearshore regions of the eastern Arabian Sea, *Ocean Sciences* 9; 343–353.

Glejin J, Sanil Kumar V, Amrutha MM, Jai Singh (2016) Characteristics of long-period swells measured in the near shore regions of eastern Arabian Sea, *International Journal of Naval Architecture and Ocean Engineering* 8: 312-319. doi: 10.1016/j.ijnaoe.2016.03.008.

Holthuijsen LH (2007) Waves in Oceanic and Coastal Waters, Cambridge University Press, Cambridge, p.387.

Joseph PV, Sooraj, KP, Rajan CK (2006) The summer monsoon onset process over South Asia and an objective method for the date of monsoon onset over Kerala. *International Journal of Climatology* 26.13: 1871-1893.

Kuik AJ, Vledder G, Holthuijsen LH (1988) A method for the routine analysis of pitch and roll buoy wave data, *J Phys Oceanogr* 18:1020–1034.

Kumar VS, Anand NM, Kumar KA, Mandal S (2003) Multi-peakedness and groupiness of shallow water waves along Indian coast, *J Coastal Res* 19:1052-1065.

Kumar VS, Johnson G, Dora GU, Philip SC, Singh J, Pednekar P (2012) Variations in nearshore waves along Karnataka, west coast of India, *J Earth Syst Sci* 121:393-403.

Kumar VS, Anand NM (2004) Variations in wave direction estimated using first and second order Fourier coefficients, *Ocean Engineering* 31: 2105–2119.

Kumar VS, Shanas PR, Dubhashi KK (2014) Shallow water wave spectral characteristics along the eastern Arabian Sea, *Natural Hazards* 70: 377–394, doi: 10.1007/s11069-013-0815-7.

Miller ST, Keim BD, Talbot RW, Mao H (2003) Sea breeze: Structure, forecasting, and impacts. *Reviews of geophysics* 1, 41(3).

Munk WH, Miller GR, Snodgrass FE, Barber NF (1963) Directional recording swell from distant storms, *Philosophical Transactions of the Royal Society, London, Series A* 255: 505-84.

Pierson WJ, Moskowitz L (1964) A proposed form for fully developed seas based on the similarity theory of S.A. Kitaigorodski, *J Geophys Res* 69: 5181-5190.

Portilla J, Ocampo-Torres FJ, Monbaliu J (2009) Spectral Partitioning and Identification of Wind Sea and Swell, *J. Atmos Ocean Tech* 26: 117-122.

Table 1. Percentage of single-peaked and multi-peaked wave spectra in different months along with classification as wind-sea dominated, swell dominated or mixed based on spectral peak period

Month	Single-peak (%)				Multi-peak (%)			
	Total	Wind-sea ($T_p < 6$)	Swell ($T_p > 8$)	Mixed (6 < $T_p < 8$)	Total	Wind-sea dominated ($T_p < 6$)	Swell dominated ($T_p > 8$)	Mixed (6 < $T_p < 8$)
January	12.03	1.14	10.82	0.07	87.97	44.35	39.78	3.83
February	18.08	1.93	16.00	0.15	81.92	45.24	29.24	7.44
March	4.57	1.95	2.28	0.34	95.43	52.82	39.92	2.69
April	4.51	0.63	2.64	1.25	95.49	41.32	21.94	32.22
May	12.10	0.27	10.49	1.34	87.90	10.56	57.23	20.11
June	80.97	0.00	80.97	0.00	19.03	0.00	18.89	0.14
July	64.65	0.00	64.65	0.00	35.35	0.00	35.35	0.00
August	47.92	0.00	47.85	0.07	52.08	0.74	45.83	5.51
September	39.10	0.14	38.47	0.49	60.90	3.33	50.97	6.60
October	25.13	0.13	25.00	0.00	74.87	14.31	58.67	1.88
November	29.38	0.49	28.89	0.00	70.63	30.00	39.72	0.90
December	26.95	0.81	26.08	0.07	73.05	23.72	41.73	7.59
Annual average	30.46	0.62	29.53	0.31	69.54	22.05	40.11	7.38

Table 2. Peak frequency, maximum spectral density of the sea surface height variance and mean wave direction at primary and secondary peak of monthly average wave spectra

Month	Primary peak			Secondary peak		
	Peak frequency (Hz)	Maximum spectral density (m ² /Hz)	Mean wave direction (deg)	Peak frequency (Hz)	Maximum spectral density (m ² /Hz)	Mean wave direction (deg)
January	0.200	0.103	295	0.075	0.063	231
February	0.220	0.105	290	0.085	0.095	225
March	0.190	0.144	283	0.065	0.085	232
April	0.160	0.190	271	0.080	0.103	225
May	0.100	0.488	230	0.160	0.284	273
June	0.090	4.309	243			
July	0.090	3.554	246			
August	0.095	1.382	243			
September	0.120	0.636	244			
October	0.080	0.150	233	0.180	0.079	266
November	0.080	0.102	232	0.230	0.047	299
December	0.100	0.182	228	0.220	0.067	298

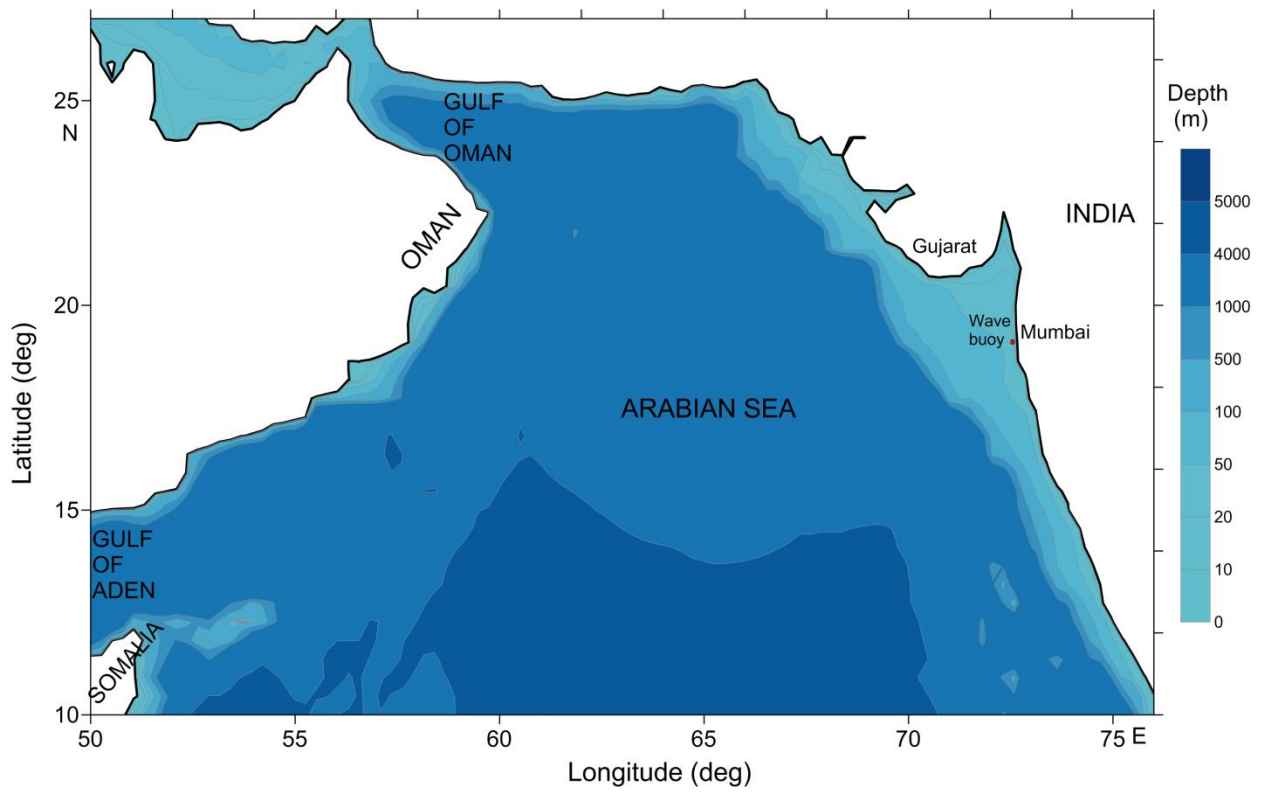


Figure 1. Map showing the wave buoy location ($19^{\circ} 7.8' N$; $72^{\circ} 44.4' E$) and the study area off Mumbai. The wave buoy is ~ 5 km away from the coast line

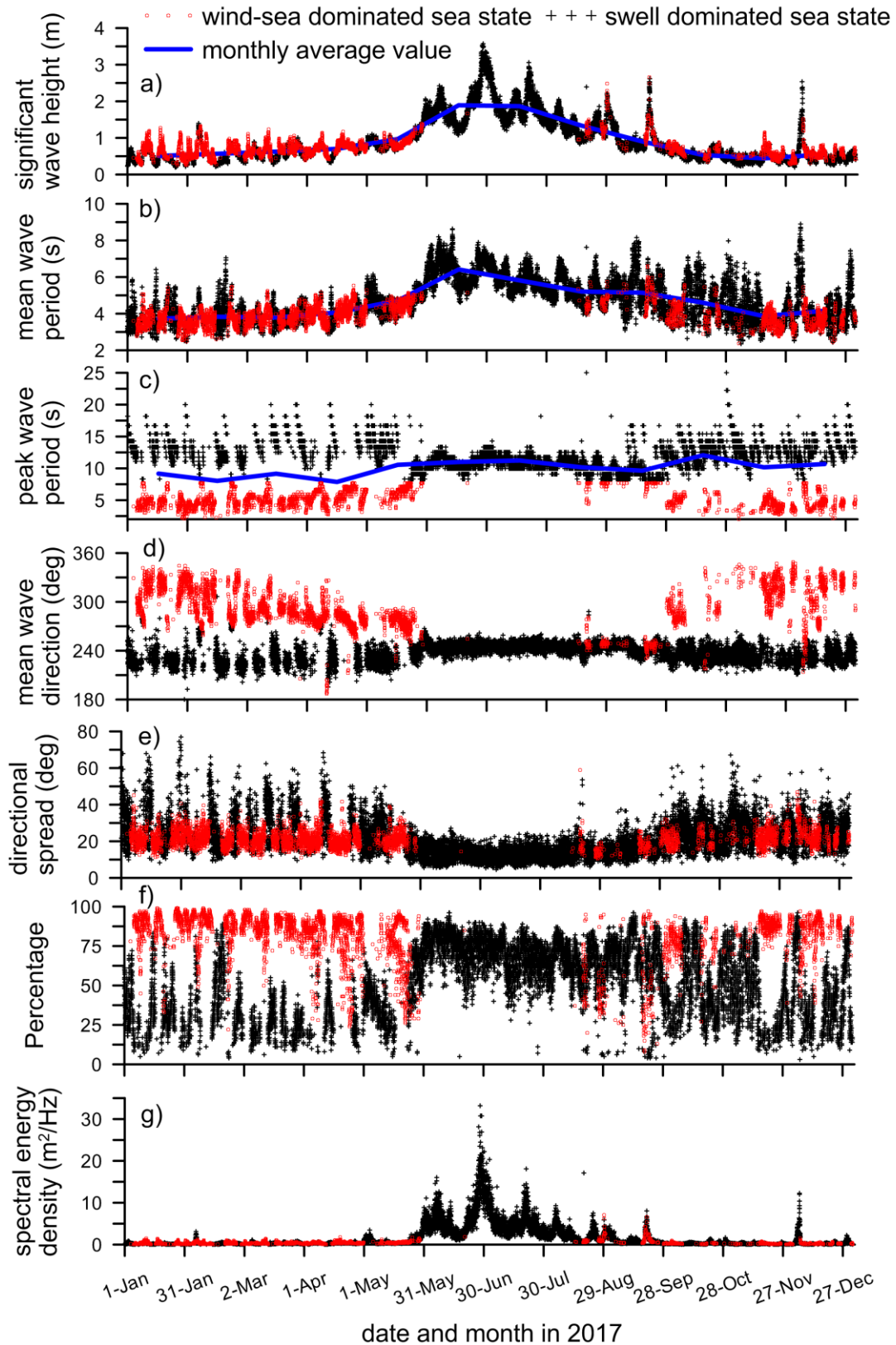


Figure 2. Time series plots of (a) significant wave height, (b) mean wave period, (c) peak wave period, (d) direction of wave, (e) wind-sea and swell contribution to the surface height variance and (f) maximum spectral density of the sea surface height variance for data covering 30 minutes. The two series shown are wind-sea dominated sea state ($T_p < 8s$) and swell dominated sea state ($T_p > 8s$). The monthly average values are also shown

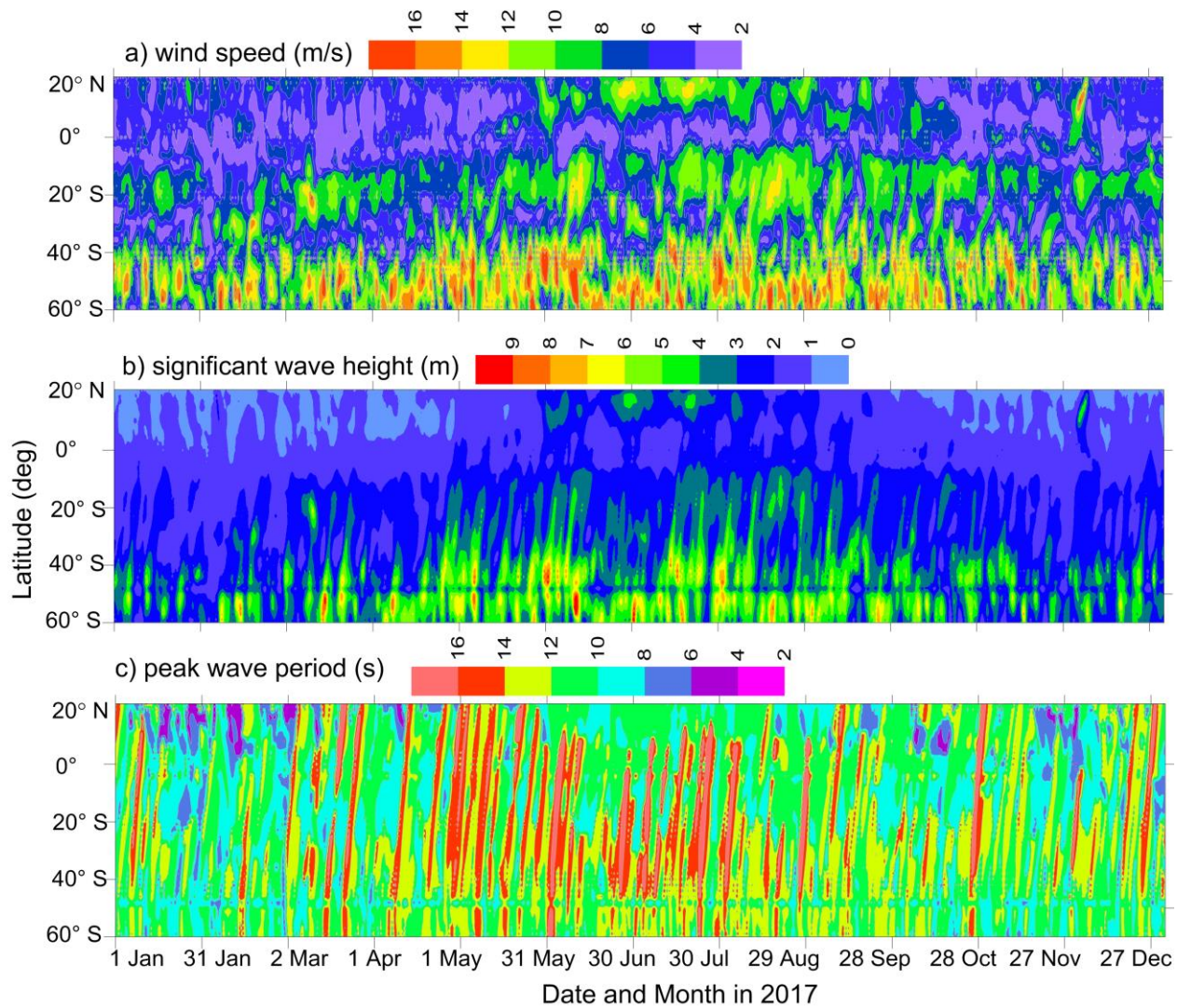


Figure 3. Latitudinal distribution of a) wind speed, b) significant wave height and c) peak wave period from 1 January to 31 December 2017 along 70.2° E longitude

(a) significant wave height (m); (b) peak wave period (s); (c) swell (%); (d) wind-sea (%)

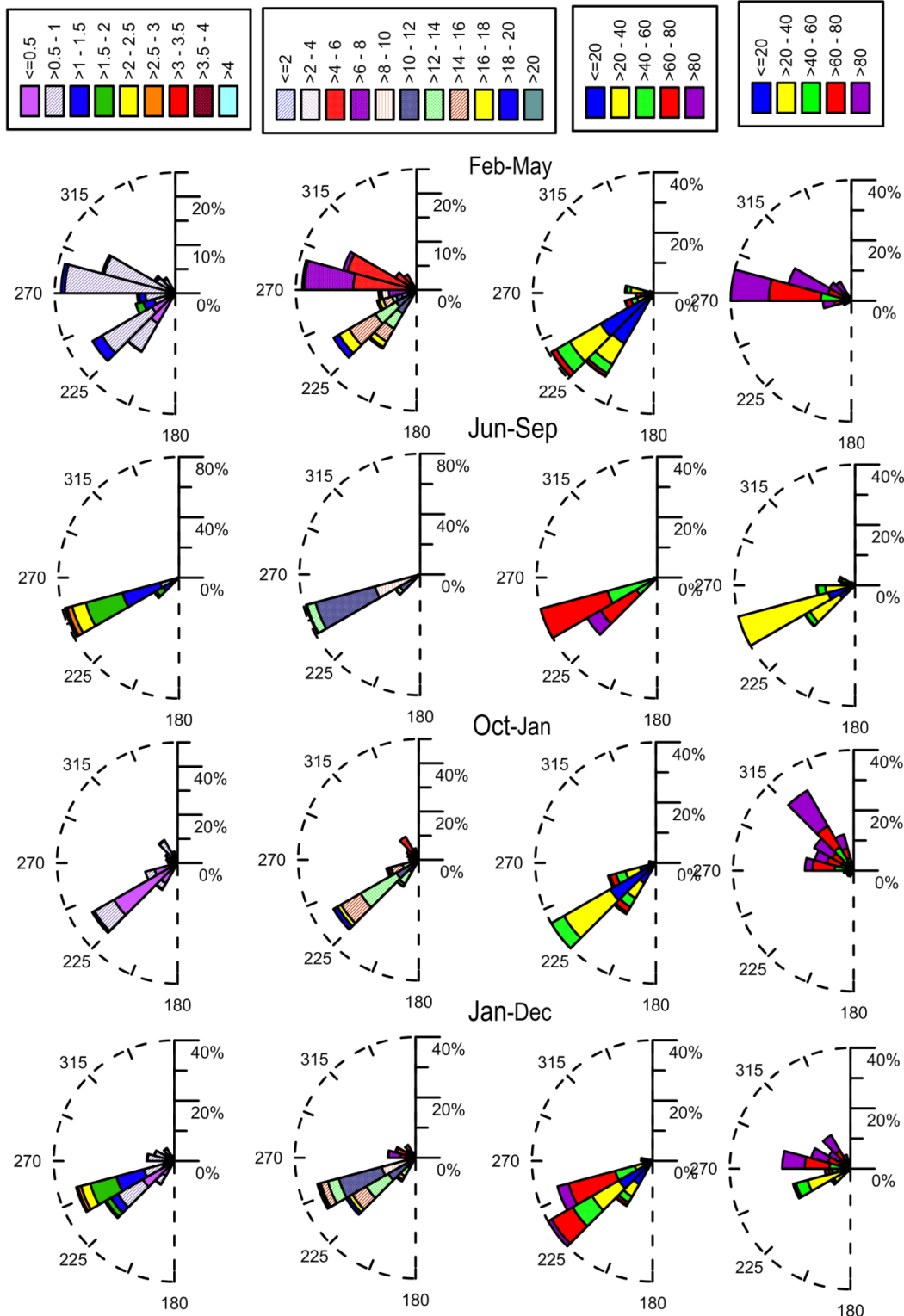
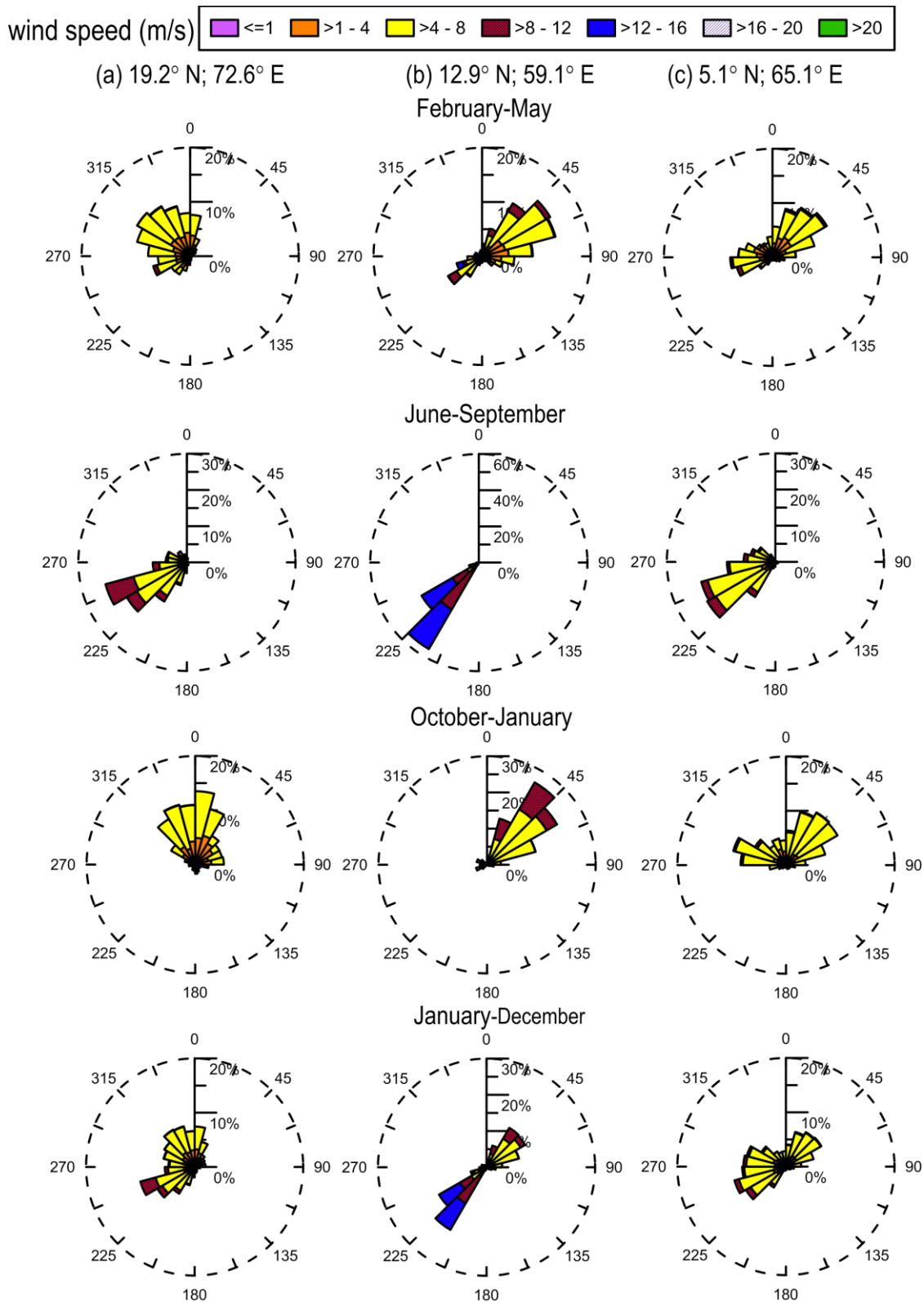


Figure 4. Wave roses during different periods 1 January 2017 to 31 December 2017 (a) significant wave height and mean wave direction, (b) peak wave period and mean wave direction, (c) percentage of swell in the measured data and mean wave direction, (d) percentage of wind-sea in the measured data and mean wave direction. The plots represent the direction of wind-sea where the waves come from. The radius of the figure indicates the percentage of the time



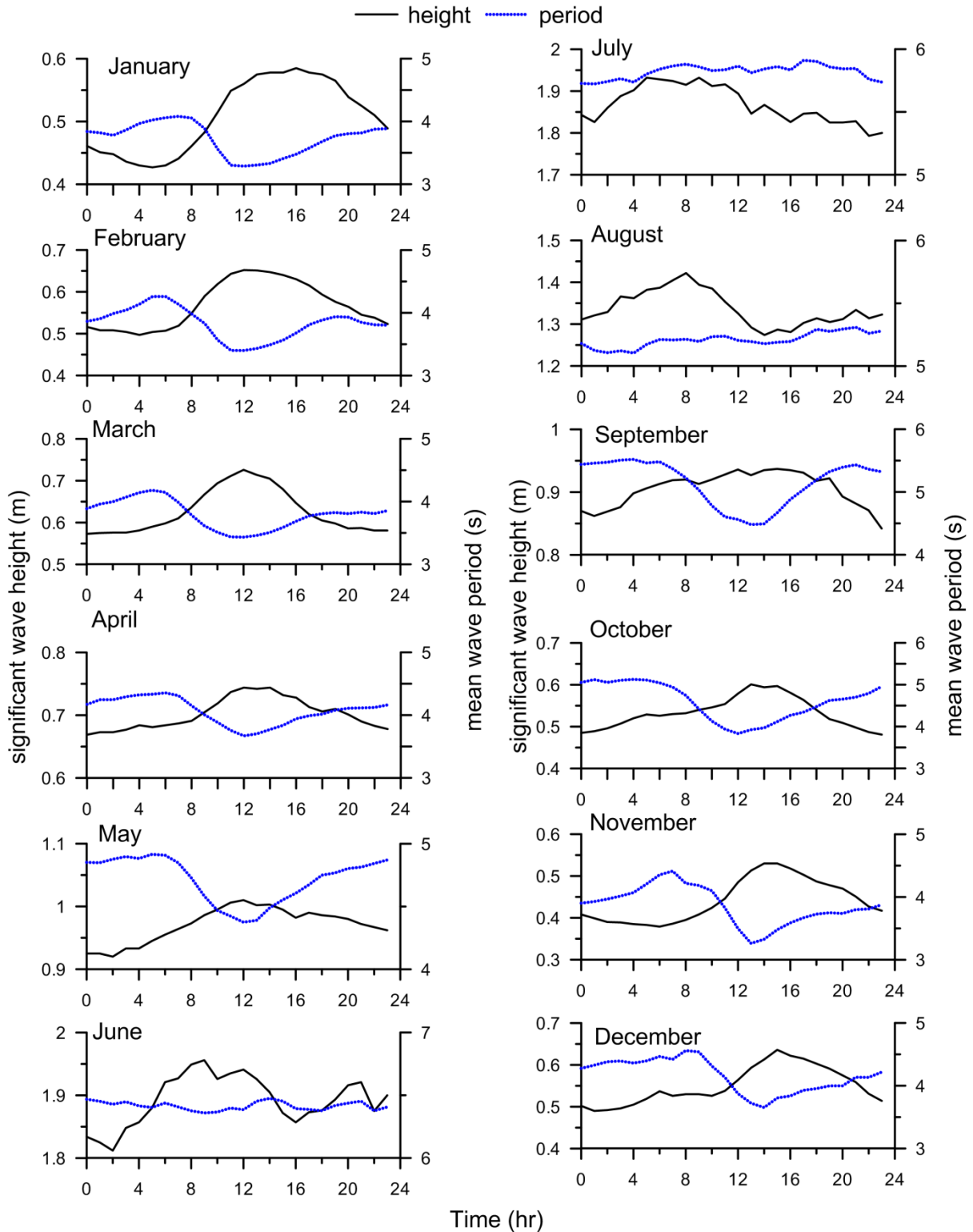


Figure 6. Variation of hourly averaged significant wave height and mean wave period in different months

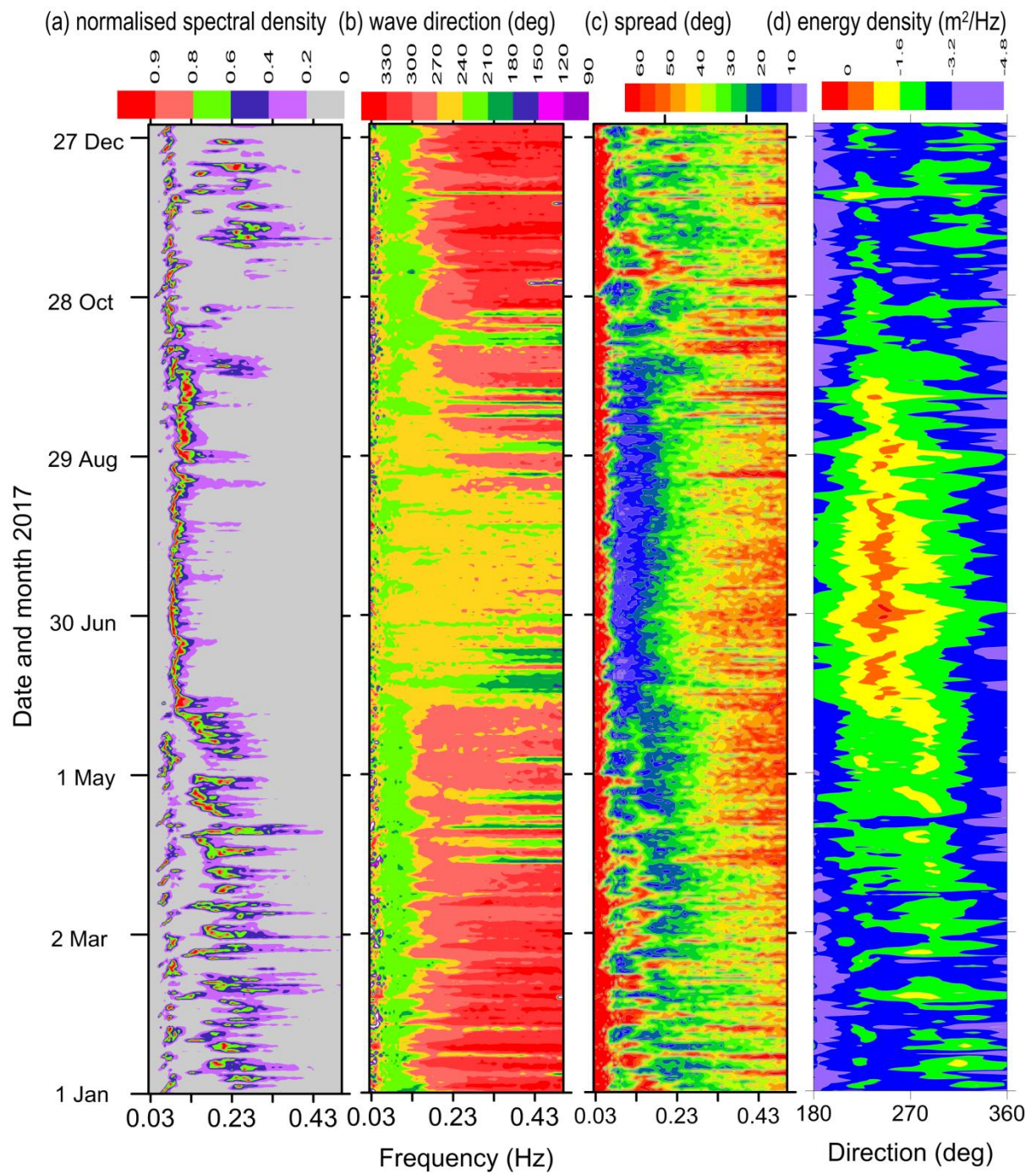


Figure 7. Contour plots of (a) normalized spectral density of the sea surface height variance, (b) mean wave direction, (c) directional spread with frequency and time, (d) contour plots of wave spectral energy density in logarithmic scale with direction and time during 1 January to 31 December 2017. Normalised spectral density of the sea surface height variance is obtained by dividing the spectral density at each frequency by the maximum spectral density of the sea surface height variance of the respective wave spectrum

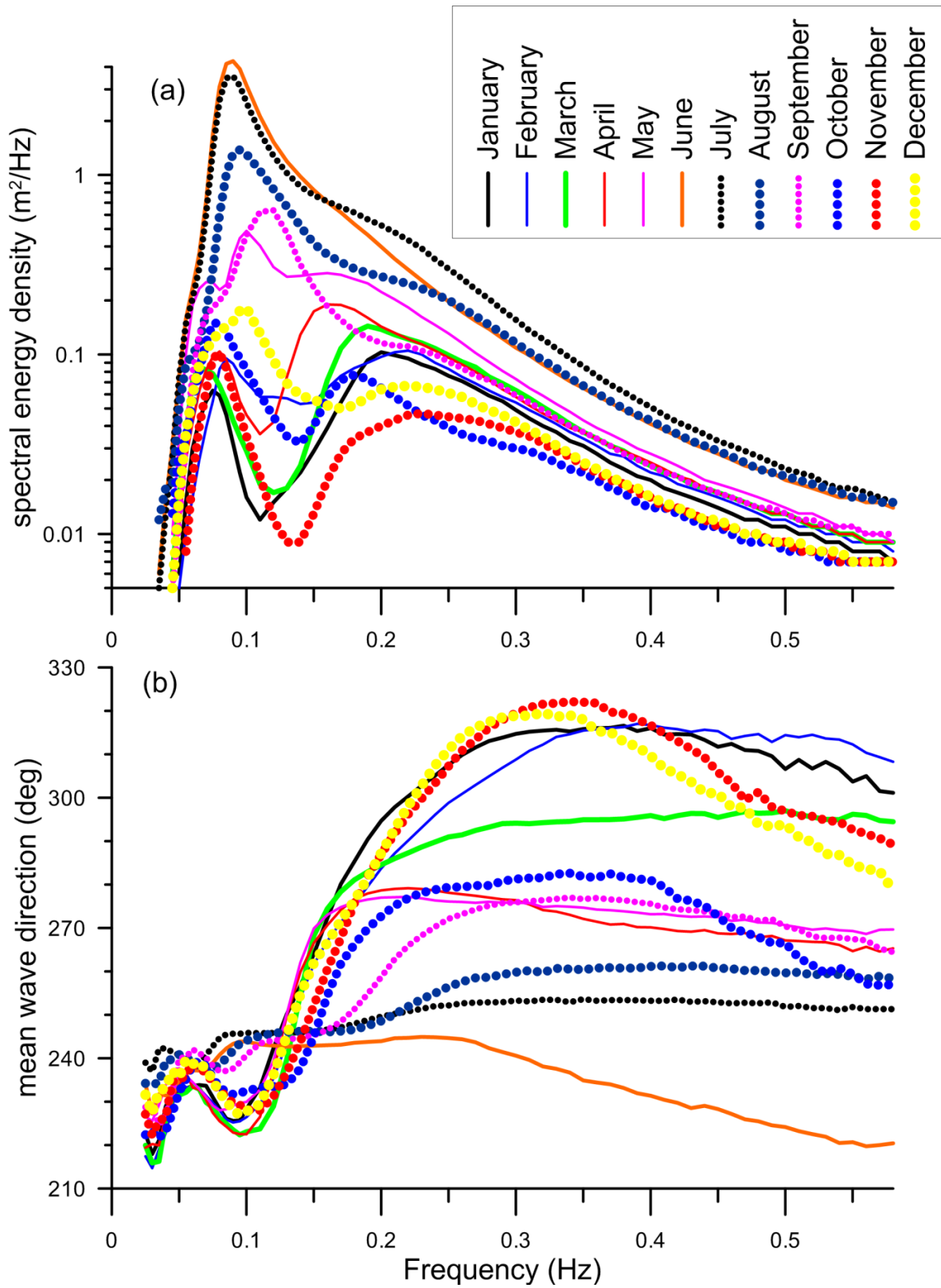


Figure 8. Monthly average wave spectrum (a) and mean wave direction (b) during January to December 2017

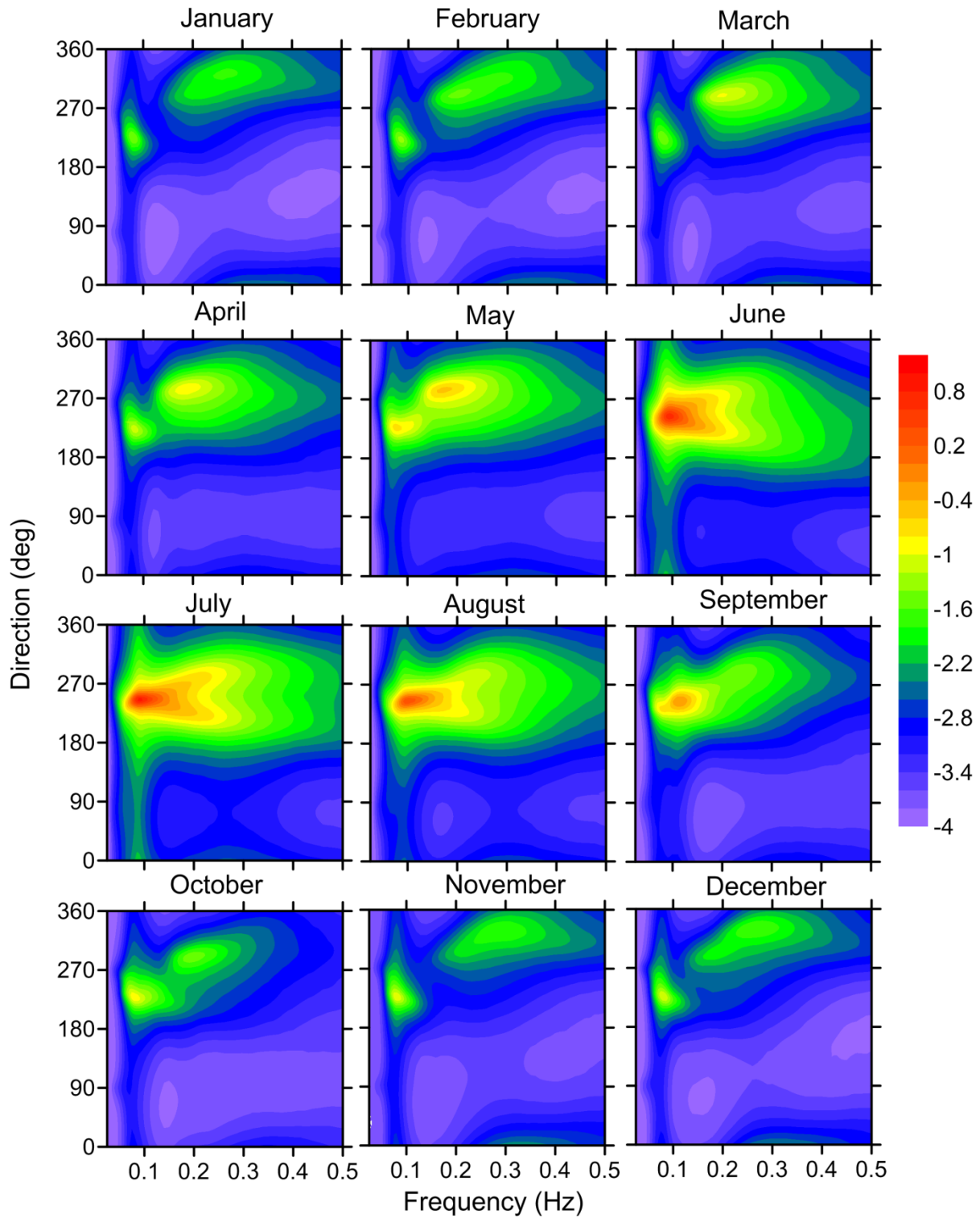


Figure 9. Monthly average directional wave spectrum during different month. The color bar is for spectral density ($\text{m}^2/\text{Deg}/\text{Hz}$). The spectral density of the sea surface height variance is shown in logarithmic scale (base 10)

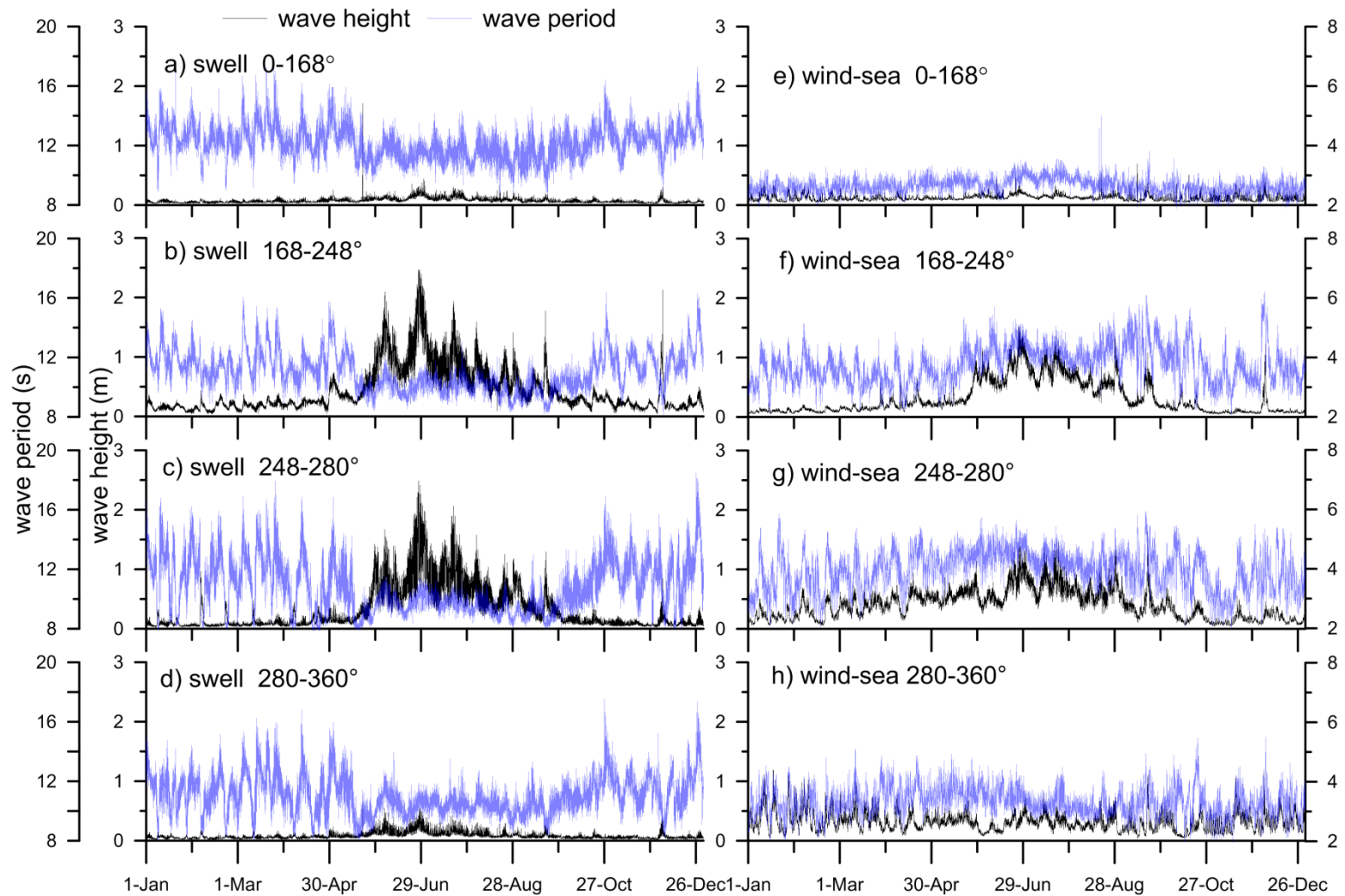


Figure 10. a-d) Significant wave height and mean wave period of swells from different direction bands (0-168°, 168-248°, 248-280° and 280-360°), e-h) corresponding significant wave height and mean wave period of wind-sea